Organometallics **1990,** *9,* 709–718

Synthesis and Reactivity of Propionyliridium Complexes. Competitive Reductive Elimination of C–H and H–H Bonds from a Propionyldihydridoiridium Complex

Paul P. Deutsch and Richard Eisenberg*

The Department of Chemistry, University of Rochester, Rochester, New York 14627

Received August 8, 1989

The complex $Ir(\eta^2\text{-}C_2H_4)(Et)(CO)(dppe)$ reacts with CO to produce initially $Ir(Et)(CO)_2(dppe)$, which then undergoes subsequent CO insertion and carbonylation to form $Ir(C(O)Et)(CO)_2(dppe)$. This latter complex was isolated and structurally characterized: space group $P\bar{1}$ (no. 2), $a = 11.046$ (2) Å, $b = 16.596$ (4) Å, $c = 8.523$ (2) Å, $\alpha = 93.93$ (2)°, $\beta = 110.94$ (2)°, $\gamma = 95.24$ (2)°, $V = 1444$ (1) Å^3, $Z = 2$. The complex $Ir(C(O)Et)(CO)_2(dppe)$ possesses a distorted trigonal-biyramidal geometry with the propionyl group in an axial position, the dppe ligand spanning the other axial and an equatorial position, and two equatorially disposed carbonyl groups. $Ir(C(O)Et)(CO)_2(dppe)$ reacts slowly with H_2 in solution to produce the complex $IrH_2(C(O)Et)(CO)(dppe)$, which has a facial arrangement of the propionyl and hydride groups. Reductive elimination of propionaldehyde with concomitant formation of $IrH_3(CO)(dppe)$ occurs at elevated temperatures under excess H_2. The kinetics of the competitive reductive eliminations of EtCHO and H_2 from $IrH_2(C(O)Et)(CO)(dppe)$ have been studied. For the reductive elimination of EtCHO, $E_{act} = 23.0 \pm 0.9$ kcal/mol, $\Delta H^{\ddagger} = 22.3 \pm 0.9$ kcal/mol, $\Delta S^{\ddagger} = -11.0 \pm 2.8$ eu, and $\Delta G^{\ddagger}(298) = 25.6 \pm 1.7$ kcal/mol. For the reductive elimination of H_2, $E_{act} = 17.1 \pm 1.6$ kcal/mol, $\Delta H^{\ddagger} = 16.5 \pm 1.6$ kcal/mol, $\Delta S^{\ddagger} = -23.3 \pm 4.8$ eu, and $\Delta G^{\ddagger}(298) = 23.4 \pm 3.0$ kcal/mol. The complex $IrH_2(C(O)Et)(CO)(dppe)$ is the first characterized example of an acyldihydridometal complex and is an intermediate in the catalytic hydroformylation of ethylene.

Introduction

The rapid growth of the field of organotransition-metal chemistry over the pass three decades has been primarily driven by the prospect of using metal complexes as catalysts for the transformation of organic compounds. During this time, a great deal of information has been accumulated about metal–carbon bonds, metal–hydrogen bonds, the interaction of metal centers with H–H and C–H bonds, and the transformations of metal-bound ligands. This information has been important in understanding the mechanism of many homogeneously catalyzed reactions.[1-3]

The hydroformylation of olefins by the catalyst precursor $RhH(CO)(PPh_3)_3$ is one of the better known examples of homogeneous catalysis in action. This intensively studied reaction is proposed to take place via a multistep sequence, Scheme I. This sequence involves the reversible dissociation of ligand, binding of the olefin, insertion of the olefin into the M–H bond, carbonylation of the alkyl group, oxidative addition of H_2, and reductive elimination from the metal center forming a C–H bond.[4] To be a useful catalyst, a metal complex must perform such a reaction sequence very rapidly. This makes any direct observation of reaction intermediates extremely difficult. Most of the steps of a catalytic sequence such as Scheme I are therefore implied from studies using model complexes or model substrates or from other related chemical reactions. However, the reductive elimination of aldehyde product from the acyl dihydride species has not been well documented, despite the fact that this is the product-forming step in the reaction.[5]

The formation of H–H and C–H bonds via reductive elimination from metal complexes has been studied for some systems,[6-17] but less so than the corresponding oxidative addition reactions. There is currently little known about the *relative* reductive elimination of H–H and C–H from organometallic complexes. This is despite the fact that the success or failure of a catalytic process, such as that shown in Scheme I, may ultimately depend upon these reductive eliminations. To gain information about relative C–H and H–H bond formation, either (a) the reductive elimination of R–H from L_nMRH and H–H from L_nMH_2 giving rise to the same L_nM fragment must be studied or (b) the reductive elimination of both H–H and R–H from the same MRH_2 complex must be studied. The latter approach will be used in the present study.

---

(1) Masters, C. *Homogeneous Transition-Metal Catalysis*; Chapman & Hall: New York, 1981.

(2) Pignolet, L. H., Ed. *Homogeneous Catalysis with Metal Phosphine Complexes*; Plenum Press: New York, 1983.

(3) Collman, J. P.; Hegedus, L. S.; Norton, J. R.; Finke, J. R. *Principles and Applications of Organotransition Metal Chemistry*; University Science Books: Mill Valley, CA, 1987.

(4) Jardine, F. H. *Polyhedron* **1982**, *1*, 569–605.

(5) We are aware of no acyl dihydride complexes in the literature. However, a few acyl monohydride complexes can be found.

(6) (a) Vaska, L.; Wernecke, M. F. *Ann. N.Y. Acad. Sci.* **1971**, *172*, 546–62. (b) Vaska, L. *Acc. Chem. Res.* **1968**, *1*, 335–44. (c) Strohmeier, W.; Muller, F. J. *Z. Naturforsch.* **1969**, *24b*, 931–2, and references therein. (d) Wink, D. A.; Ford, P. C. *J. Am. Chem. Soc.* **1986**, *108*, 4838–42.

(7) Packett, D. L.; Trogler, W. C. *Inorg. Chem.* **1988**, *27*, 1768–75.

(8) (a) Abis, L.; Sen, A.; Halpern, J. *J. Am. Chem. Soc.* **1978**, *100*, 2915–6. (b) Michelin, R. A.; Faglia, S.; Ugiagliati, P. *Inorg. Chem.* **1983**, *22*, 1831–4.

(9) (a) Wax, M. J.; Stryker, J. M.; Buchanan, J. M.; Kovac, C. A.; Bergman, R. G. *J. Am. Chem. Soc.* **1984**, *106*, 1121–2. (b) Buchanan, J. M.; Stryker, J. M.; Bergman, R. G. *J. Am. Chem. Soc.* **1986**, *108*, 1537–50, and references therein.

(10) (a) Jones, W. D.; Feher, F. J. *J. Am. Chem. Soc.* **1984**, *106*, 1650–63, and references therein. (b) Periana, R. A.; Bergman, R. G. *J. Am. Chem. Soc.* **1986**, *108*, 7332–46, and references therein. (c) Jones, W. D.; Feher, F. J. *Organometallics* **1983**, *2*, 562–3.

(11) (a) Bullock, R. M.; Headford, C. E. L.; Kegley, S. E.; Norton, J. R. *J. Am. Chem. Soc.* **1985**, *107*, 727–9. (b) Giannotti, C.; Green, M. L. H. *J. Chem. Soc., Chem. Commun.* **1972**, 114–6.

(12) Milstein, D. *J. Am. Chem. Soc.* **1982**, *104*, 5227–8.

(13) McAlister, D. R.; Erwin, D. K.; Bercaw, J. E. *J. Am. Chem. Soc.* **1978**, *100*, 5966–8.

(14) (a) Okrasinski, S. J.; Norton, J. R. *J. Am. Chem. Soc.* **1977**, *99*, 295–7. (b) Evans, J.; Norton, J. R. *J. Am. Chem. Soc.* **1974**, *96*, 7577–8.

(15) (a) Balazs, A. C.; Johnson, K. H.; Whitesides, G. M. *Inorg. Chem.* **1982**, *21*, 2162–74. (b) Obara, S.; Kitaura, K.; Morokuma, K. *J. Am. Chem. Soc.* **1984**, *106*, 7482–92.

(16) Chan, A. C. S.; Halpern, J. *J. Am. Chem. Soc.* **1980**, *102*, 838–40.

(17) Thorn, D. L. *Organometallics* **1982**, *1*, 197–204.

0276-7333/90/2309-0709$02.50/0

Scheme I

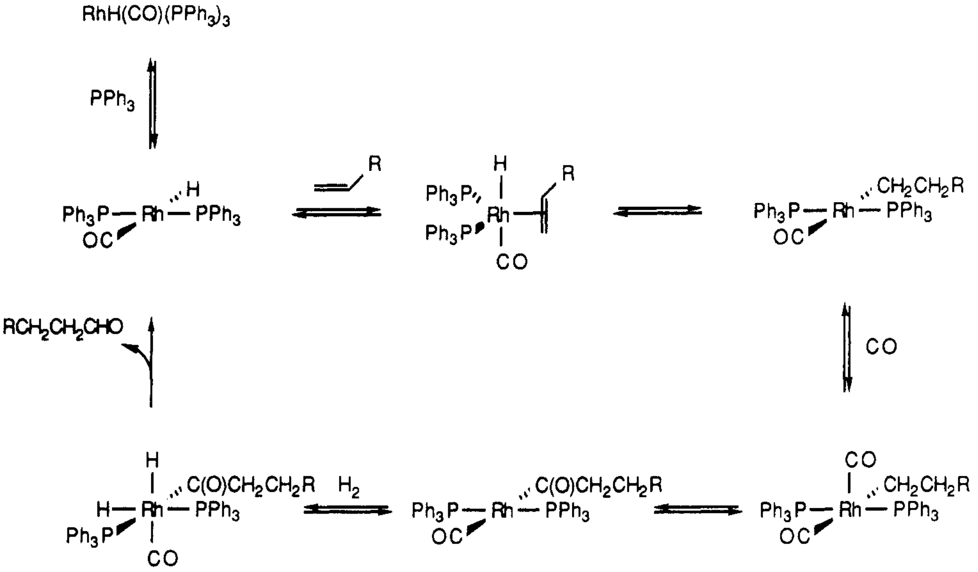

We have recently reported on the synthesis and reactivity of $Ir(\eta^2-C_2H_4)(Et)(CO)(dppe)$ and $IrH_2(Et)(CO)(dppe)$.[18] The latter complex was found to undergo competitive reductive elimination of ethane and hydrogen, with H_2 elimination being more favorable. We now describe the synthesis and characterization of $Ir(Et)(CO)_2(dppe)$, $Ir(C(O)Et)(CO)_2(dppe)$, and $IrH_2(C(O)Et)(CO)(dppe)$ and the competitive reductive elimination of EtCHO and H_2 from the last of these complexes.

Results

Reaction of $Ir(Et)(\eta^2-C_2H_4)(CO)(dppe)$ with CO. A rapid reaction occurs between carbon monoxide and solutions of $Ir(Et)(\eta^2-C_2H_4)(CO)(dppe)$, 1, which liberates C_2H_4 and produces a new complex 2 in less than 5 min (eq 1). This new complex, 2, is formulated as $Ir(Et)(CO)_2(dppe)$ on the basis of the spectroscopic characterization and reaction chemistry to be discussed below. Small amounts of a second complex, 3, are also observed.

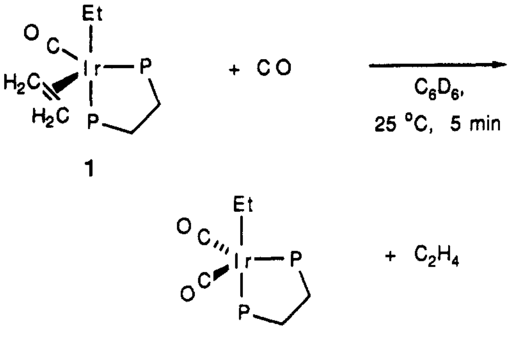

1

2

The ^1H NMR spectrum of 2 contains a single *o*-phenyl resonance at δ 7.536 (8 H), a broad multiplet at δ 1.97 (4 H), and two multiplets at δ 2.174 and 2.09 (3 H and 2 H, respectively). These last two multiplets are not present in $Ir(C_2D_5)(CO)_2(dppe)$, 2-d_5, formed from $Ir(\eta^2-C_2D_4)(C_2D_5)(CO)(dppe)$, 1-$d_9$, and CO and are therefore assigned to a σ-ethyl ligand. The single *o*-phenyl resonance and the broad dppe ethylene resonance indicate that 2 is a fluxional species.

$Ir(Et)(CO)_2(dppe)$ exhibits two broadened resonances in the $^{31}P\{^1H\}$ NMR spectrum at room temperature. These resonances shift slightly as toluene solutions of 2 are cooled to −40 °C but are not frozen out.[19] The infrared spectrum of 2 in benzene-d_6 contains two absorptions between 2200 and 1500 cm^{-1} attributed to ν_{CO} at 1965 and 1916 cm^{-1},[20] whereas only one metal–carbonyl resonance is observed in the ^{13}C NMR spectrum of ^{13}CO-labeled 2, formed from 1-(^{13}CO) and ^{13}CO.[21]

The static structure for $Ir(Et)(CO)_2(dppe)$, 2, shown in eq 1, is drawn as a trigonal bipyramid since a five-coordinate d^8 Ir(I) species would most likely adopt this geometry.[22] The spectroscopic data for 2 indicate that the two carbonyl groups are equivalent, whereas the two ends of the chelating phosphine ligand are not. Since the dppe ligand does not readily span two equatorial positions in a trigonal bipyramid,[23] it can be assumed to occupy one axial and one equatorial site. This would then place the two carbonyl ligands in equatorial positions and the ethyl ligand in an axial position. This is in keeping with theoretical treatments that suggest that stronger η^2-acid ligands prefer equatorial sites in a d^8 trigonal bipyramid, whereas better σ-donors prefer axial sites.[24,25] The spectroscopic data also indicate that 2 is stereochemically nonrigid,[19] being in the fast exchange limit of the ^1H NMR time scale but in the slow exchange limit of the slightly faster ^{31}P NMR time scale (the time scale difference is inversely related to the chemical shift difference in hertz between exchanging nuclei).[26]

The ethyl dicarbonyl complex 2 is not the end product of the reaction of 1 with carbon monoxide. Over a period

---

[18] Deutsch, P. P.; Eisenberg, R. *J. Am. Chem. Soc.* **1990**, *112*, 714.

[19] Mann, B. E. In *Comprehensive Organometallic Chemistry*; Wilkinson, G., Ed.; Pergammon: Oxford, 1982; Vol. 3, Chapter 20.

[20] Nakamoto, K. *Infrared and Raman Spectra of Inorganic and Coordination Compounds*, 4th ed.; Wiley: New York, 1986.

[21] Mann, B. E.; Taylor, B. F. *^{13}C NMR Data for Organometallic Compounds*; Academic: New York, 1981.

[22] Huheey, J. E. *Inorganic Chemistry*; 2nd ed.; Harper & Row: New York, 1978; Chapter 10, pp 432–7.

[23] McAuliffe, C. A.; Levason, W. *Phosphine, Arsine, and Stilbine Complexes of the Transition Elements*; Elsevier: New York, 1979; pp 212–4, and references therein.

[24] Mingos, D. M. P. In *Comprehensive Organometallic Chemistry*; Wilkinson, G., Ed.; Pergammon: Oxford, 1982; Vol. 3; Chapter 19.

[25] Rossi, A. R.; Hoffman, R. *Inorg. Chem.* **1975**, *14*, 365, and references therein.

[26] From ref 19, the rate of two-site exchange if $k = 2^{-1/2}\pi\Delta\nu$. For 2 to show equivalent *o*-phenyl resonances, the rate of exchange would have to be ≥450 s^{-1}, assuming $\nu_A - \nu_b$ = 200 Hz (0.5 ppm) in a static structure. To coalesce two ^{31}P NMR resonances separated by 800 Hz (~5 ppm; see low-temperature data for 2), the rate of exchange would have to be 1800 s^{-1}.

Table I. Summary of Crystallographic Data for $Ir(C(O)Et)(CO)_2(dppe)$, 3

empirical formula	$IrP_2O_3C_{31}H_{29}$
formula wt	703.74
cryst system	triclinic
lattice parameters	
a, Å	11.046 (2)
b, Å	16.596 (4)
c, Å	8.523 (2)
α, deg	93.93 (2)
β, deg	110.94 (2)
γ, deg	95.24 (2)
V, Å^3	1444 (1)
space group	$P\bar{1}$ (no. 2)
Z	2
d(calc), g/cm^3	1.62
$F(000)$	692
abs coeff μ(Mo Kα), cm^{-1}	50.44
diffractometer	Enraf-Nonius CAD4
radiation	Mo Kα (λ = 0.71069 Å, graphite monochromated)
temp, °C	23
2θ(max), deg	43.9
no. observations ($I > 3\theta(I)$)	3123
no. variables	334
residuals R, R_w	0.020, 0.025
GOF indicator	0.99
max shift in final cycle	0.35
largest peak in final diff map, e$^-$/Å^3	0.69

Table II. Positional and Isotropic Thermal Parameters and Their Estimated Standard Deviations for $Ir(C(O)Et)(CO)_2(dppe)$, 3[a]

atom	x	y	z	B(eq), Å^2
IR	0.20846 (2)	0.23127 (1)	0.01512 (2)	2.674 (8)
P1	0.2299 (1)	0.15736 (8)	0.2490 (2)	3.18 (4)
P2	0.3624 (1)	0.32710 (8)	0.2167 (1)	3.07 (4)
O1	0.3000 (4)	0.1077 (2)	−0.1798 (5)	5.9 (2)
O2	−0.0680 (4)	0.2628 (3)	−0.0349 (7)	7.4 (2)
O3	0.3068 (4)	0.3083 (2)	−0.2216 (5)	4.9 (2)
C1	0.2656 (5)	0.1529 (3)	−0.1011 (6)	3.7 (2)
C2	0.0383 (5)	0.2516 (3)	−0.0148 (7)	4.1 (2)
C3	0.2197 (4)	0.3072 (3)	−0.1680 (6)	3.2 (2)
C4	0.1168 (5)	0.3636 (3)	−0.2347 (7)	4.6 (2)
C5	0.1461 (7)	0.4270 (4)	−0.335 (1)	7.5 (3)
C6	0.3536 (5)	0.3077 (3)	0.4208 (6)	3.8 (2)
C7	0.3532 (4)	0.2172 (3)	0.4361 (6)	3.8 (2)
C11	0.2960 (5)	0.0599 (3)	0.2530 (6)	3.6 (2)
C12	0.2371 (5)	−0.0103 (3)	0.2846 (7)	4.8 (2)
C13	0.2939 (7)	−0.0820 (4)	0.2854 (8)	6.0 (3)
C14	0.4081 (7)	−0.0826 (4)	0.2587 (8)	6.1 (3)
C15	0.4671 (6)	−0.0123 (4)	0.2266 (8)	5.9 (3)
C16	0.4118 (5)	0.0588 (3)	0.2244 (7)	4.8 (2)
C21	0.0840 (4)	0.1343 (3)	0.2969 (6)	3.3 (2)
C22	0.0786 (5)	0.1521 (4)	0.4545 (7)	4.6 (2)
C23	−0.0347 (6)	0.1282 (4)	0.4824 (8)	6.1 (3)
C24	−0.1416 (5)	0.0899 (4)	0.3548 (8)	5.6 (3)
C25	−0.1389 (5)	0.0733 (4)	0.1966 (7)	4.7 (2)
C26	−0.0267 (5)	0.0958 (3)	0.1677 (6)	4.2 (2)
C31	0.5345 (4)	0.3231 (3)	0.2502 (6)	3.4 (2)
C32	0.5676 (5)	0.2750 (3)	0.1360 (6)	4.0 (2)
C33	0.6978 (5)	0.2681 (4)	0.1645 (8)	5.4 (3)
C34	0.7930 (5)	0.3092 (5)	0.303 (1)	6.5 (3)
C35	0.7616 (5)	0.3572 (5)	0.4166 (8)	6.6 (3)
C36	0.6321 (5)	0.3644 (4)	0.3901 (7)	5.0 (2)
C41	0.3388 (4)	0.4339 (3)	0.1989 (6)	3.5 (2)
C42	0.2201 (5)	0.4577 (3)	0.1962 (7)	4.7 (2)
C43	0.1927 (6)	0.5355 (4)	0.1677 (8)	5.6 (3)
C44	0.2821 (7)	0.5913 (4)	0.1446 (8)	5.9 (3)
C45	0.3986 (6)	0.5688 (3)	0.1476 (8)	5.4 (3)
C46	0.4276 (5)	0.4901 (3)	0.1741 (7)	4.1 (2)

[a] Values for anisotropically refined atoms are given in the form of the isotropic equivalent thermal parameter defined as $^4/_3[a^2B(1,1) + b^2B(2,2) + c^3B(3,3) + ab(\cos\gamma)B(1,2) + ac(\cos\beta)B(1,3) + bc(\cos\alpha)B(2,3)]$. Estimated standard deviations in the least significant figure are given in parentheses.

Table III. Selected Bond Distances and Angles in $Ir(C(O)Et)(CO)_2(dppe)$, 3[a]

	Distances, Å		
Ir–C1	1.869 (5)	P2–C6	1.825 (5)
Ir–C2	1.870 (5)	P2–C31	1.827 (5)
Ir–C3	2.102 (5)	O1–C1	1.150 (6)
Ir–P2	2.327 (1)	O2–C2	1.159 (6)
Ir–P1	2.363 (1)	O3–C3	1.203 (5)
P1–C21	1.814 (5)	C3–C4	1.514 (7)
P1–C11	1.831 (5)	C4–C5	1.481 (8)
P1–C7	1.835 (5)	C6–C7	1.517 (7)
P2–C41	1.824 (5)		
	Angles, deg		
C1–Ir–C2	129.5 (2)	C7–P1–Ir	107.6 (2)
C1–Ir–C3	86.1 (2)	C41–P2–C6	104.9 (2)
C1–Ir–P2	119.0 (2)	C41–P2–C31	105.2 (2)
C1–Ir–P1	95.2 (1)	C41–P2–Ir	117.2 (2)
C2–Ir–C3	92.6 (2)	C6P2–C31	103.3 (2)
C2–Ir–P2	111.3 (2)	C6–P2–Ir	106.8 (2)
C2–Ir–P1	93.8 (2)	C31–P2–Ir	117.9 (2)
C3–Ir–P2	87.5 (1)	O1–C1–Ir	176.0 (4)
C3–Ir–P1	170.6 (1)	O2–C2–Ir	178.8 (5)
P2–Ir–P1	83.71 (5)	O3–C3–C4	118.1 (4)
C21–P1–C11	103.9 (2)	O3–C3–Ir	122.0 (4)
C21–P1–C7	107.4 (2)	C4–C3–Ir	119.9 (3)
C21–P1–Ir	116.8 (2)	C5–C4–C3	116.4 (5)
C11–P1–C7	101.7 (2)	C7–C6–P2	108.7 (3)
C11–P1–Ir	118.2 (2)	C6–C7–P1	111.2 (3)

[a] Estimated standard deviations in the least significant figure are given in parentheses.

of hours, 2 disappears as a second product, 3, grows in. This conversion follows first-order kinetics with $k_{obs} = 1.293 \times 10^{-4}$ s^{-1} at 25.7 °C under an excess of CO.[27] When this reaction is performed under ^{13}CO, incorporation of labeled CO into 2 is competitive with conversion to 3. The ^{13}C NMR spectra show some label in the Ir—C≡O resonance of 2 and in the EtC(O)–Ir resonance of 3.

The spectroscopic data indicate that 3 is Ir(C(O)Et)(CO)$_2$(dppe), the result of CO insertion into the metal–ethyl bond followed by carbonylation, as shown in eq 2.[28]

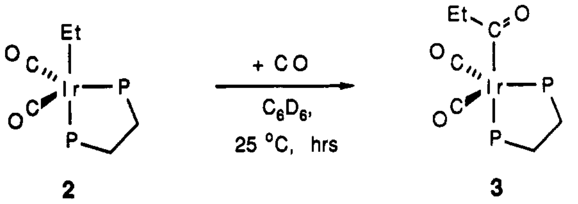

(2)

The most striking features in the ^1H NMR spectrum of this complex are a downfield quartet at δ 2.830 and a triplet at δ 0.858 that are coupled to one another. Similar ^1H NMR resonances have been observed for other acyl complexes.[29] The ^1H NMR spectrum of 3 also contains dppe resonances.

Two broadened resonances are present in the $^{31}P\{^1H\}$ NMR spectrum of 3. These resonances shift upon cooling,

---

(27) (a) Atwood, J. D. *Inorganic and Organometallic Reaction Mechanisms*; Brooks/Cole, Monterey, CA, 1985. (b) Moore, J. W.; Pearson, R. G. *Kinetics and Mechanism*; 3rd ed.; Wiley-Interscience: New York, 1981. (c) Unweighted least-squares fit of lines with error analysis from algorithms in: Bevington, P. R. *Data Reduction and Error Analysis for the Physical Sciences*; McGraw-Hill: New York, 1969; Chapter 6, pp 117–8.

(28) (a) Calderazzo, F. *Angew. Chem., Int. Ed. Engl.* **1977**, *16*, 294–9. (b) See also Chapter 6 in ref 3.

(29) See, for example: (a) Yagupsky, C.; Brown, C. K.; Wilkinson, G. *J. Chem. Soc., Dalton Trans.* **1970**, 1392–1401, and references therein. (b) Rees, W. M.; Churchill, M. R.; Atwood, J. D. *Organometallics* **1985**, *4*, 1164–7. (c) Schwartz, J.; Cannon, J. B. *J. Am. Chem. Soc.* **1972**, *94*, 6226–8. (d) Collman, J. P.; Vastine, F. D.; Roper, W. R. *J. Am. Chem. Soc.* **1968**, *90*, 2282–7. (e) Kubota, M.; Blake, D. M. *J. Am. Chem. Soc.* **1971**, *93*, 1368–73.

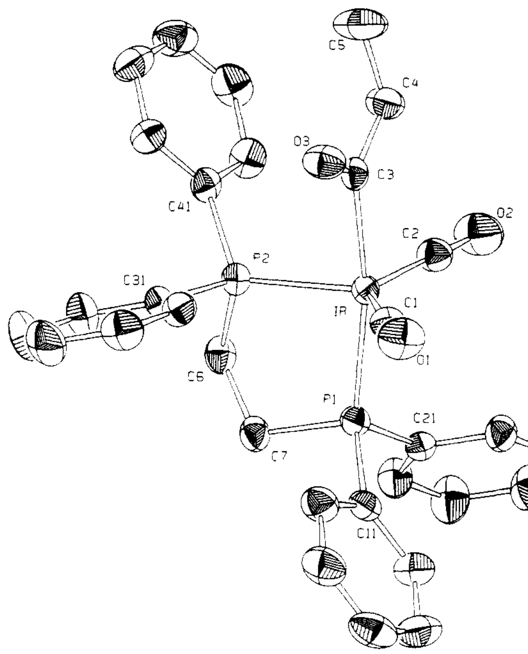

Figure 1. ORTEP plot of $Ir(C(O)Et)(CO)_2(dppe)$, **3**, shown with 35% probability thermal ellipsoids. Hydrogen atoms are omitted for clarity.

in a behavior similar to that of 2, described earlier. The $^{13}C\{^1H\}$ NMR spectrum of the ^{13}CO-labeled complex contains two resonances, δ 186.81 and 215.35, in an approximately 2 to 1 ratio. The former resonance is appropriate for a terminal Ir–CO while the latter is shifted downfield, as expected for an acyl carbonyl group.[21] The infrared spectrum of 3 shows three carbonyl stretches, ν_{CO}, at 1977, 1929, and 1635 cm^{-1}, all of which shift to lower energy in 3-$(^{13}CO)_3$. The low-energy IR absorption is typical of acyl carbonyl stretches.[29,30]

It proved possible to prepare and isolate 3 with elemental analysis in agreement with the formulation of the complex as $Ir(C(O)Et)(CO)_2(dppe)$. Crystals were grown from saturated toluene solutions of 3 at low temperature and were analyzed by single-crystal X-ray diffraction. An ORTEP plot of $Ir(C(O)Et)(CO)_2(dppe)$ is shown in Figure 1, and selected structural data are listed in Tables I–III. The complex adopts a distorted trigonal-bipyramidal geometry, with the propionyl group occupying an axial position and the two carbonyl groups occupying equatorial sites. The structural arrangement is in accord with theoretical treatments on bonding in d^8 trigonal-bipyramidal complexes in having the better π-acid carbonyl ligands in equatorial positions and the σ-donor acyl ligand in an equatorial site.[24,25,31] The Ir–P distances are normal, 2.363 (axial) and 2.327 Å (equatorial), as are the Ir–C(carbonyl) distances, 1.869 and 1.870 Å. The angles about the sp^2-hybridized acyl carbon (C3) are 118.1, 119.9, and 122.0°. The Ir–C(acyl) bond distance (2.102 Å) is longer than that found for $Ir(C(O)CH_2CMe_3)(PPh_3)_2(MeOC(O)C{\equiv}CCOOMe)$, 1.915 Å,[32] but is in closer agreement with the value found in $Ir(C(O)OMe)(CO)_2(PPh_3)_2$, 2.073 Å.[33] The solid-state structure of 3 is strikingly similar to those found for $IrH(CO)_2(PPh_3)_2$,[34] $Ir(C(O)OMe)(CO)_2(PPh_3)_2$,[33] and $Co(C(O)R)(CO)_2(dppe)$, R = CH(OEt)CH(OEt)Me.[35] All of these complexes adopt distorted trigonal-bipyramidal geometries with two equatorial carbonyl groups and an axial hydride or acyl group.

Reaction of $Ir(C(O)Et)(CO)_2(dppe)$, 3, with H_2. A slow reaction occurs between benzene solutions of 3 and hydrogen at room temperature. This reaction cleanly produces a new complex, 4, as indicated in eq 3. The ^{1}H NMR spectrum of 4 contains two hydride resonances, δ −8.473 and −8.795, a propionyl methyl resonance, and two diastereotopic methylene resonances.[36] These are in addition to the dppe-based signals. On the basis of spectroscopic characterization, 4 is the propionyl dihydride complex $IrH_2(C(O)Et)(CO)(dppe)$. This complex can be prepared in bulk and isolated as an analytically pure white powder in 72% yield.

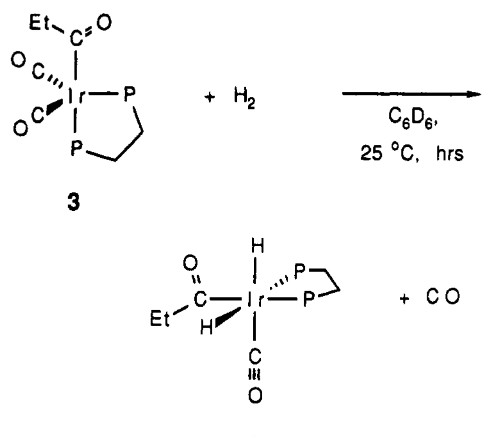

(3)

The $^{31}P\{^1H\}$ NMR spectrum of 4 contains resonances for the dppe ligand, the the ^{13}C NMR spectrum of ^{13}CO-enriched 4 contains resonances for the carbonyl and propionyl ligands. The infrared spectrum of 4 contains absorptions due to ν_{Ir-H} and ν_{CO} from both the metal-bound terminal carbonyl ligand and the carbonyl group of the propionyl ligand.

The structure of 4, shown in eq 3, is conclusively determined from the spectroscopic data. The couplings observed in the ^{1}H, ^{31}P, and ^{13}C NMR spectra indicate that one hydride is trans to a phosphine, while the other hydride is cis to both phosphines and trans to the terminal carbonyl.[18,21,37,38] Coupling of ν_{CO} and ν_{Ir-H} also indicates that the carbonyl is trans to a hydride ligand.[37,39] The configuration of the ligands around the iridium center in 4 is the same as that found for $IrH_2(Et)(CO)(dppe)$[18] and the kinetic isomers of $IrH_2X(CO)(dppe)$, X = Cl, Br, I, CN.[40]

$IrH_2(C(O)Et)(CO)(dppe)$ is stable as a solid or in solution under H_2. However, 4 is observed to undergo a slow decomposition in solution under vacuum or nitrogen at

---

(30) See ref 3, p 107.

(31) Blackburn, B. K.; Davies, S. G.; Sutton, K. H.; Whittaker, M. *Chem. Soc. Rev.* **1988**, *17*, 147–79.

(32) Rappoli, B. J.; Churchill, M. R.; Janik, T. S.; Rees, W. M.; Atwood, J. D. *J. Am. Chem. Soc.* **1987**, *109*, 5145–9.

(33) Churchill, M. R.; Fettinger, J. C.; Rees, W. M.; Atwood, J. D. *J. Organomet. Chem.* **1986**, *304*, 227–38.

(34) Ciechanowicz, M.; Skapski, S. C.; Troughton, P. G. H. *Acta Crystallogr.* **1976**, *B32*, 1673–80.

(35) Tso, C. C.; Cutler, A. R. *J. Am. Chem. Soc.* **1987**, *109*, 5844–5.

(36) Becker, E. D. *High Resolution NMR*, 2nd ed.; Academic: New York, 1980; Chapter 7, pp 174–8.

(37) (a) Moore, D. S.; Robinson, S. D. *Chem. Soc. Rev.* **1983**, *12*, 415–52. (b) Kaesz, H. D.; Saillant, R. B. *Chem. Rev.* **1972**, *72*, 231–281. () Jesson, J. P. In *Transition Metal Hydrides*; Muetterties, E. L., Ed.; Marcel-Dekker: New York, 1971; Chapter 4.

(38) Jameson, C. J. In *Phosphorus-31 NMR Spectroscopy in Stereochemical Analysis*; Verkade, J. G., Quin, L. D., Eds.; VCH Publishers: Deerfield, FL, 1987; Chapter 6.

(39) Vaska, L. *J. Am. Chem. Soc.* **1966**, *88*, 4100–1.

(40) (a) Fisher, B. J.; Eisenberg, R. *Organometallics* **1983**, *2*, 764–7. (b) Fisher, B. J.; Eisenberg, R. *Inorg. Chem.* **1984**, *23*, 3216–22. (c) Johnson, C. E.; Fisher, B. J.; Eisenberg, R. *J. Am. Chem. Soc.* **1983**, *105*, 7772–4.

room temperature that results in mixtures containing $IrH_3(CO)(dppe)$,[40] $IrH(CO)_2(dppe)$,[40] $IrH_2Et(CO)(dppe)$,[18] $Ir(C(O)Et)(CO)_2(dppe)$, EtCHO, C_2H_6, and C_2H_4.

The clean formation of $IrH_3(CO)(dppe)$, **5**, and EtCHO is observed when solutions of **4** are heated under excess H_2 (eq 4). Some incorporation of D_2 into **4** prior to elimination of propionaldehyde is observed when this reaction is performed under D_2. This suggests that reductive elimination of H_2 is competitive with propionaldehyde reductive elimination. The rates of these reactions proved amenable to kinetic studies, and a series of experiments were performed to investigate the relative rates of these two reductive eliminations.

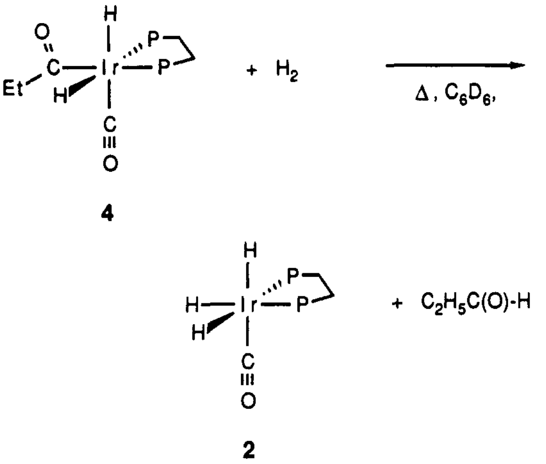

(4)

The reaction shown in eq 4 does not appear to be reversible. When solutions of $IrH_3(CO)(dppe)$ were heated with EtCHO (up to 90 °C, 24 h), no **4** or products that might result from formation of **4** are observed. No deuterium or labeled carbon monoxide is incorporated into the EtCHO when the same reaction is performed under D_2 or ^{13}CO.

Kinetics of Reductive Elimination of EtCHO and H_2 from 4. Two different reductive eliminations from $IrH_2(C(O)Et)(CO)(dppe)$, **4**, producing either EtCHO or H_2 are possible due to the facial disposition of the propionyl and hydride ligands (eq 5). This is analogous to the internally competitive reductive eliminations of C_2H_6 and H_2 from $IrH_2(Et)(CO)(dppe)$ reported by us previously.[18] The competitive EtC(O)–H and H–H reductive eliminations from **4** were studied quantitatively because of (a) the uniqueness of this well-characterized acyl dihydride complex,[5] (b) the relative paucity of alkyl dihydride complexes and their reaction chemistry,[41-44] and (c) the interesting activation parameters found for the analogous $IrH_2(Et)(CO)(dppe)$ system.[18]

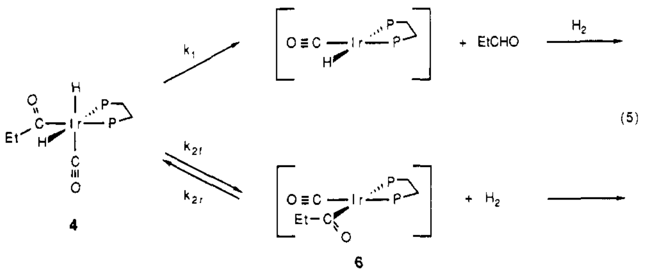

The overall rate equation for eq 5 is shown in eq 6.[27] Reactions were performed under an excess of H_2 to determine the rate constant for the elimination of EtCHO, k_1. No complex such as **6** or a secondary product arising from **6** was observed under these reactions, which allowed for the use of the steady-state approximation for [**6**], d[**6**]/dt = 0. This leads to the simple first-order differential and integrated rate laws shown in eqs 7 and 8, respectively.

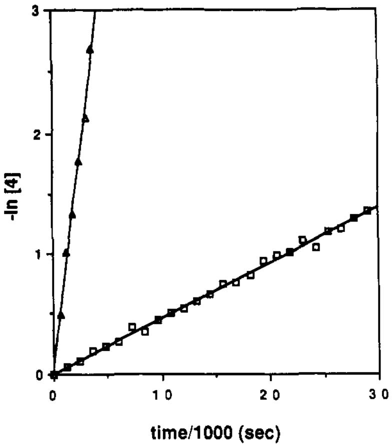

Figure 2. Representative kinetic data for reductive elimination of EtCHO (□) and $C_2H_5CHO + H_2$ (△) from $IrH_2(C(O)Et)(CO)(dppe)$, **4**, at 57.7 °C.

Table IV. Rate Constants for the Reductive Elimination of EtCHO and H_2 from $IrH_2(C(O)Et)(CO)(dppe)$[a]

temp, °C	10^4k_1, s^{-1}	10^4k_{obs}, s^{-1}	10^4k_{2f}, s^{-1}
50.2	0.220 ± 0.003	3.99 ± 0.14	3.77 ± 0.14
57.7	0.460 ± 0.006[b]	8.29 ± 0.15[c]	7.83 ± 0.16[d]
66.7	1.312 ± 0.040[e]	15.12 ± 0.19	13.81 ± 0.23
75.7	2.813 ± 0.052	*f*	

[a] Reaction conditions: [**4**] = 5 mM in C_6D_6, and 700 Torr of H_2 or D_2 added at −196 °C. Values are least-squares fit of lines from plots of −ln [**4**] vs time, according to refs 27a and 27c. Errors (1 standard deviation) also according to ref 27c. [b] With [**4**] = 1.2 mM, $k_1 = (0.377 \pm 0.021) \times 10^{-4}\ s^{-1}$. With only 175 Torr of H_2 added at −196 °C, $k_1 = (0.450 \pm 0.089) \times 10^{-4}\ s^{-1}$. [c] With [**4**] = 1.2 mM, $k_{obs} = (10.53 \pm 1.30) \times 10^{-4}\ s^{-1}$. With 175 Torr of D_2 added at −196 °C, $k_{obs} = (6.943 \pm 0.55) \times 10^{-4}\ s^{-1}$. Reaction with CO instead of D_2, $k_{obs} = (8.321 \pm 0.19) \times 10^{-4}\ s^{-1}$. [d] From reaction with CO, $k_{2f} = (7.86 \pm 0.20) \times 10^{-4}\ s^{-1}$. [e] Duplicate run at 66.7 °C, $k_1 = (1.363 \pm 0.026) \times 10^{-4}\ s^{-1}$. [f] Too fast for accurate measurement.

$$-d[\mathbf{4}]/dt = (k_1 + k_{2f})[\mathbf{4}] - k_{2r}[H_2][\mathbf{6}] \tag{6}$$

$$-d[\mathbf{4}]/dt = k_1[\mathbf{4}] \tag{7}$$

$$-\ln([\mathbf{4}]/[\mathbf{4}]_0) = k_1 t \tag{8}$$

The reductive elimination of EtCHO from **4** under an excess of H_2 was followed by ^1H NMR spectroscopy over the temperature range 50.2–75.7 °C. The decay of the hydride resonances from **4** and growth of hydride resonances of the $IrH_3(CO)(dppe)$ product (**5**) follow simple first-order kinetics.[27] Plots of −ln ([**4**]/[**4**]$_0$) vs time were linear for at least 2 half-lives. Representative kinetic data are shown in Figure 2, and the measured rate constants, k_1, are listed in Table IV. The reductive elimination of EtCHO from **4** occurs with $k_1 = (1.312 \pm 0.040) \times 10^{-4}\ s^{-1}$ at 57.7 °C. The elimination of EtC(O)–D from $IrD_2(C(O)Et)(CO)(dppe)$, **4**-d_2, occurs with $k_1 = (0.927 \pm 0.030) \times 10^{-4}\ s^{-1}$ at 57.7 °C, giving a normal kinetic isotope effect of $k_H/k_D = 1.4 \pm 0.1$. The rate of propionaldehyde elimination is not affected by varying the concentrations of **4** or H_2.

To obtain the rate constant for reductive elimination of H_2 from **4**, k_{2f}, the reductive elimination of H_2 from **4** was performed under D_2. Under these conditions, any **6** formed would react with D_2 to form **4**-d_2, eliminating the reverse reaction to regenerate **4**-d_0 by the k_{2r} pathway. The rate

Table V. Activation Parameters for the Reductive Elimination of EtCHO and H_2 from $IrH_2(C(O)Et)(CO)(dppe)$, 4[a]

activation parameter	$H-C(O)C_2H_5$ elimination	H-H elimination
E_{act}, kcal/mol	23.0 ± 0.9	17.1 ± 1.6
$\log_{10} A$, s^{-1}	10.9 ± 0.6	8.2 ± 1.0
$\Delta H^‡$, kcal/mol	22.3 ± 0.9	16.5 ± 1.6
$\Delta S^‡$, eu	-11.0 ± 2.8	-23.3 ± 4.8
$\Delta G^‡_{298}$, kcal/mol	25.6 ± 1.7	23.4 ± 3.0

[a] Using data from reactions with [2] = 5 mM in C_6D_6, and 700 Torr of H_2 or D_2 added at -196 °C. Values shown are from least-squares fits of Arrhenius and Eyring plots according to refs 27a and 27c.

equation for these reactions under D_2 is shown in eq 9, and the integrated rate law is shown in eq 10. Since k_1 was obtained from the previous experiments performed under H_2, k_{2f} can be calculated.

$$-d[4]/dt = (k_1 + k_{2f})[4] \tag{9}$$

$$-\ln([4]/[4]_0) = (k_1 + k_{2f})t \tag{10}$$

The reductive elimination of H_2 from 4 was again monitored by ^1H NMR spectroscopy. The decay of the hydride resonances of 4 followed first-order kinetics under an excess of D_2. Plots of $-\ln([4]/[4]_0)$ vs time were linear for at least 2 half-lives, provided that the sample was shaken to ensure that the concentration of dissolved D_2 far exceeded the solution concentration of liberated H_2. Representative kinetic data are shown in Figure 2, and the observed rate constants, k_{obs}, are listed in Table IV. The observed rate constant in these experiments, k_{obs}, is the sum of the individual rate constants k_1 and k_{2f}. A kinetic isotope effect of 1.5 ± 0.1 was found for H_2 elimination from 4 by studying the reaction of 4-d_2 with H_2, yielding $k_{obs} = (10.67 \pm 0.51) \times 10^{-4}$ s^{-1} and $k_{2f} = (9.34 \pm 0.58) \times 10^{-4}$ s^{-1} at 66.7 °C. Varying the concentration of 4 and D_2 did not significantly influence the values of k_{obs}.

To double check the rate of reductive elimination of H_2 from 4, reactions were performed under a CO atmosphere. The decay of hydride resonances of 4 again followed first-order kinetics, and a plot of $-\ln([4]/[4]_0)$ vs time was linear, with k_{obs} equal to $(8.32 \pm 0.19) \times 10^{-4}$ s^{-1} at 57.7 °C. No incorporation of ^{13}CO into 4 *prior* to reductive elimination of H_2 or EtCHO was observed when the reaction was performed under ^{13}CO.

Activation parameters for the reductive elimination of EtCHO and H_2 from 4 were determined from the temperature dependence of the rate constants k_1 and k_{2f}, respectively.[27] Arrhenius plots were linear and gave the values for E_{act} listed in Table V. Eyring plots were also linear, Figure 3, and gave values for $\Delta H^‡$ and $\Delta S^‡$ that are presented in Table V. While E_{act} and $\Delta H^‡$ were in the expected range for this type of reaction, $\Delta S^‡$ for both reductive eliminations were relatively large and negative, indicating an ordered transition state for these reactions.

Discussion

Formation of $Ir(Et)(CO)_2(dppe)$, 2, and $Ir(C(O)Et)(CO)_2(dppe)$, 3. The lability of the ethylene ligand in $Ir(Et)(\eta^2-C_2H_4)(CO)(dppe)$, 1, has previously been established.[18] When a solution of 1 is placed under CO, ethylene is readily displaced by carbon monoxide to produce an ethyl dicarbonyl complex $Ir(Et)(CO)_2(dppe)$, 2. Complex 2 slowly undergoes CO insertion and subsequent carbonylation to form $Ir(C(O)Et)(CO)_2(dppe)$, 3.

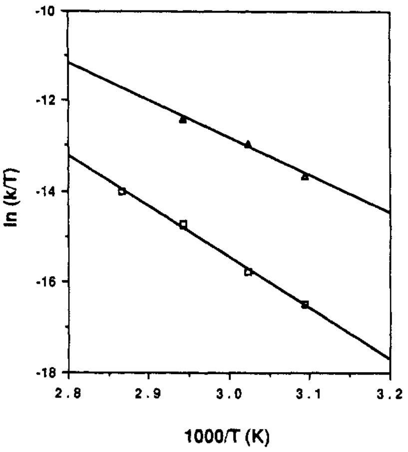

Figure 3. Eyring plots for reductive elimination of EtCHO (□) and H_2 (△) from $IrH_2(C(O)Et)(CO)(dppe)$, 4.

The formulation of the initial new complex 2 as $Ir(Et)(CO)_2(dppe)$ is based upon spectroscopic characterization of 2 and comparison of 2 to the final product of the reaction with CO, 3. Complex 2 is similar to the previously characterized iridium complexes $IrX(CO)_2(dppe)$, X = H, Br, or I.[40] These three complexes are fluxional, and the halide complexes rapidly exchange CO.

$Ir(Et)(CO)_2(dppe)$ most likely forms by a simple dissociative substitution of CO for C_2H_4 (eq 11), in accord with

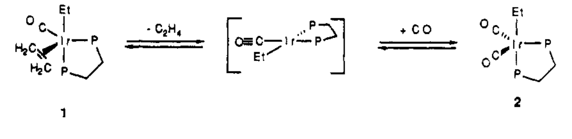

(11)

the previously reported C_2H_4/C_2D_4 exchange studies on 1 that showed the lability of the ethylene ligand.[18] Since 1 is an 18-electron complex, a dissociative pathway is most likely, with the 16-electron intermediate [Ir(Et)(CO)(dppe)] reacting rapidly with CO to give 2. This ethyl monocarbonyl species was previously proposed to be an intermediate along the path to the formation of 1 from $IrH_3(CO)(dppe)$ and C_2H_4 and in the formation of $IrH_2(Et)(CO)(dppe)$.[18]

$Ir(Et)(CO)_2(dppe)$ is not stable and slowly converts to $Ir(C(O)Et)(CO)_2(dppe)$, 3. This complex is the result of CO insertion into the Ir–Et bond (or ethyl migration to CO) followed by reaction of the resulting species with CO (eq 12).

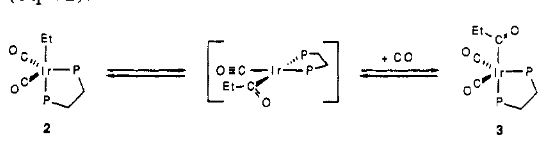

(12)

Spectroscopic data were initially used to identify 3 as a propionyl complex. Confirmation for the formulation of 3 as the propionyl dicarbonyl complex came from the X-ray structure determination. This study revealed a trigonal bipyramidal coordination geometry with an axial propionyl ligand and dppe spanning axial and equatorial sites. The spectroscopic data for $Ir(C(O)Et)(CO)_2(dppe)$ are for the most part consistent with the solid-state structural data but indicate some stereochemical nonrigidity.

The reversibility of the reactions shown in eq 12 is indicated by (a) subsequent reaction of 3 with H_2 to form 4 and (b) the decomposition of solutions of 3 upon gentle heating to form $IrH(CO)_2(dppe)$ and C_2H_4. The first observation indicates that the CO trapping step in eq 12 is reversible, while the second suggests that the reaction steps are reversible all the way back to [Ir(Et)(CO)(dppe)] and even [IrH(CO)(dppe)]. Specifically, CO "deinsertion" from the complex Ir(C(O)(Et)(CO)(dppe) forms Ir(Et)$(CO)_2$(dppe). Loss of CO from this species generates the intermediate [Ir(Et)(CO)(dppe)], which can undergo β-elimination and loss of C_2H_4 to give [IrH(CO)(dppe)]. This unstable species is then trapped by CO to form IrH$(CO)_2$(dppe).

The two carbonyl complexes Ir(Et)$(CO)_2$(dppe) and Ir(C(O)Et)$(CO)_2$(dppe) are similar to species involved in homogeneous hydroformylation reactions catalyzed by RhH(CO)$(PPh_3)_3$[4] and other monohydride catalysts.[1-3] This chemistry is analogous to the landmark catalysis studies on IrH(CO)L$(PPh_3)_2$ and RhH(CO)L$(PPh_3)_2$ investigated by Wilkinson 20 years ago.[29a] In one of these studies, Wilkinson observed Ir(C(O)Et)$(CO)_2(PPh_3)_2$, Ir(C(O)Et)(CO)$(PPh_3)_2$ and Ir(Et)$(CO)_2(PPh_3)_2$, Ir(Et)(CO)$(PPh_3)_2$ spectroscopically in the reaction of C_2H_4 and CO with IrH$(CO)_2(PPh_3)_2$.[29a] These studies also provided evidence for some of the intermediates proposed in RhH(CO)$(PPh_3)_3$-catalyzed hydrogenation and hydroformylation. The reaction of CO with IrMe(CO)$(PPh_3)_2$ to produce sequentially IrMe$(CO)_2(PPh_3)_2$ and Ir(C(O)Me)$(CO)_2(PPh_3)_2$ has also been well characterized.[29b-e]

Formation of IrH_2(C(O)Et)(CO)(dppe), 4. A slow reaction occurs between 3 and hydrogen at room temperature giving rise to the new complex IrH_2(C(O)Et)(CO)(dppe), 4. This complex was identified on the basis of IR and NMR spectroscopic data, elemental analysis, and reaction chemistry. The spectroscopic data also provided enough information to assign unambiguously the geometry of the complex. The disposition of the ligands around the metal center in 4 is the same as that proposed for IrH_2(Et)(CO)(dppe),[18] and the kinetic H_2 oxidative addition products IrH_2X(CO)(dppe), X = H, Cl, Br, I, CN.[40] There was no evidence for the presence of any other stereoisomer of 4.

Complex 4 is unique as an acyl dihydride complex. We are aware of no other stable, isolable acyl dihydride complexes even though these species are frequently proposed as intermediates in the hydroformylation of olefins by monohydride catalysts such as RhH(CO)$(PPh_3)_3$. However, a number of related alkyl dihydride complexes have been reported,[41-44] as have several acyl monohydride species.[45-49] For example, the acyl hydrides *cis*-FeH(C(O)Et)$(dmpe)_2$ and cis-FeH(C(O)Ph)$(dmpe)_2$ are produced by reaction of propionaldehyde and benzaldehyde, respectively, with the species [Fe$(dmpe)_2$], which was generated in situ by elimination of naphthalene from Fe(Np)H$(dmpe)_2$.[45] The formyl hydride complexes IrH(C(O)H)$(PMe_3)_3$Cl, IrH(C(O)H)(Me)$(PMe_3)_3$, and IrH(C(O)H)$(PMe_3)_4^+$ form by oxidative addition of H_2CO to IrCl$(PMe_3)_3(Me_2CO)$, Ir(Me)$(PMe_3)_4$, and Ir$(PMe_3)_4^+$, respectively.[17] Some related methoxycarbonyl complexes were also reported in this study. Similarly, the reaction of H_2CO or MeCHO with $Os(CO)_2(PMe_3)_3$ was found to produce OsH(C(O)H)$(CO)_2(PMe_3)_2$ or OsH(C(O)Me)$(CO)_2(PMe_3)_2$ via oxidative addition to the intermediate [$Os(CO)_2(PMe_3)_2$].[46] A number of other hydrido acyl complexes have been made by an intramolecular oxidative addition of an aldehydic C–H bond which is part of a bound ligand[47] and by other chemical transformations.[48]

Reductive Elimination of H_2 and EtCHO from IrH_2(C(O)Et)(CO)(dppe). Two different reductive eliminations from 4 are possible due to the fac disposition of the propionyl and two hydride ligands. Both of these reductive eliminations are observed to occur. While there is only one path for H–H elimination, shown as A, there are in principle two different ways in which EtC(O)–H can be eliminated from 4, B and C. Of the two pathways, only B is likely to occur as a concerted process. Path C would require the phosphines to move to mutually trans positions, which is not possible for the dppe ligand. The similarity of the paths for H_2 and EtCHO reductive elimination allows a direct comparison of the kinetic parameters of these paths to be made. These reductive eliminations were therefore studied in detail to gain insight into the relative tendency to undergo H–H vs H–acyl reductive elimination from the Ir(III) center.

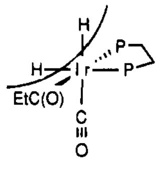

A

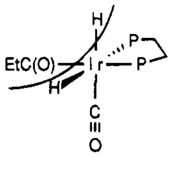

B

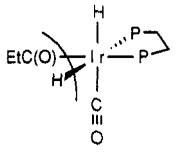

C

Elimination of H_2 from 4 is found to be more facile than EtCHO elimination. Hydrogen elimination also occurs more readily than ethane elimination from IrH_2(Et)(CO)(dppe).[18] Both of these observations are in contrast to the generally accepted notion that C–H reductive elimination from a metal complex is faster than H–H reductive elimination.

The activation parameters for the reductive elimination of EtCHO and H_2 from 4 were determined from the reaction rate constants using Arrhenius and Eyring plots. The activation parameters for R–H and H–H elimination from IrH_2(C(O)Et)(CO)(dppe) and IrH_2(Et)(CO)(dppe) are similar.

The values for $\Delta H^\ddagger$ for EtC(O)–H and Et–H elimination from IrH_2(C(O)Et)(CO)(dppe) and IrH_2(Et)(CO)(dppe) are 22.3 ± 0.9 and 20.2 ± 0.4 kcal/mol, respectively. This possibly reflects a slightly stronger Ir–C(O)Et bond relative to the Ir–Et bond. The values for $\Delta S^\ddagger$ for EtC(O)–H and Et–H elimination are very close to one another at −11.0 ± 2.8 and −10.9 ± 1.3 eu, respectively. The negative values for $\Delta S^\ddagger$ indicate that the transition states for both R–H eliminations are ordered. The similarity of these values may also reflect a similarity in the structure of the transition states. Both reductive eliminations also have a normal primary kinetic isotope effect, k_H/k_D (R–H/R–D) = 1.4 ± 0.1 (EtC(O)–H) and 2.4 ± 0.1 (Et–H), indicating some net weakening of the bonds involving H in the transition state. Values for k_H/k_D greater than unity are typical for simple, concerted reductive elimination of R–H from metal complexes.[8]

The reductive elimination of H_2 from IrH_2(C(O)Et)(CO)(dppe) and from IrH_2(Et)(CO)(dppe) shows very similar activation parameters, with $\Delta H^\ddagger$ of 16.5 ± 1.6 and 15.5 ± 1.1 kcal/mol and $\Delta S^\ddagger$ of −23.3 ± 4.8 and −23.7 ±

---

(41) Burk, M. J.; McGrath, M. P.; Wheeler, R.; Crabtree, R. *J. Am. Chem. Soc.* **1988**, *110*, 5034–9.

(42) Hirsekorn, F. J.; Rakowski, R. C.; Muetterties, E. L. *J. Am. Chem. Soc.* **1975**, *97*, 237–8.

(43) Strope, D.; Shriver, D. F. *J. Am. Chem. Soc.* **1973**, *95*, 8197–8.

(44) Longato, B.; Bresadola, S. *Inorg. Chem.* **1982**, *21*, 168–73.

(45) Tolman, C. A.; Ittel, S. D.; English, A. D.; Jesson, J. P. *J. Am. Chem. Soc.* **1979**, *101*, 1742–51.

(46) (a) Headford, C. E. L.; Roper, W. R. *J. Organomet. Chem.* **1980**, *198*, C7-10. (b) Brown, K. L.; Clark, G. R.; Headford, C. E. L.; Marsden, K.; Roper, W. R. *J. Am. Chem. Soc.* **1979**, *101*, 503–5.

(47) (a) Suggs, J. W. *J. Am. Chem. Soc.* **1978**, *100*, 640–1. (b) Suggs, J. W.; Pearson, G. D. N. *Tetrahedron Lett.* **1980**, *21*, 3853–6. (c) Rauchfuss, T. B. *J. Am. Chem. Soc.* **1979**, *101*, 1045–7. (d) Landvatter, E. F.; Rauchfuss, T. B. *Organometallics* **1982**, *1*, 506–13.

(48) (a) Milstein, D. *Acc. Chem. Res.* **1984**, *17*, 221–6, and references therein. (b) Francis, B. R.; Green, M. L. H.; Luong-thi, T.; Moser, G. A. *J. Chem. Soc., Dalton Trans.* **1976**, 1339–45. (c) Ibekwe, S. D.; Taylor, K. A. *J. Chem. Soc. A* **1970**, 1–3.

(49) Perrin, D. D.; Armarego, W. L. F.; Perrin, D. R. *Purification of Laboratory Chemicals*, 2nd ed.; Pergammon Press: New York, 1980.

Scheme II

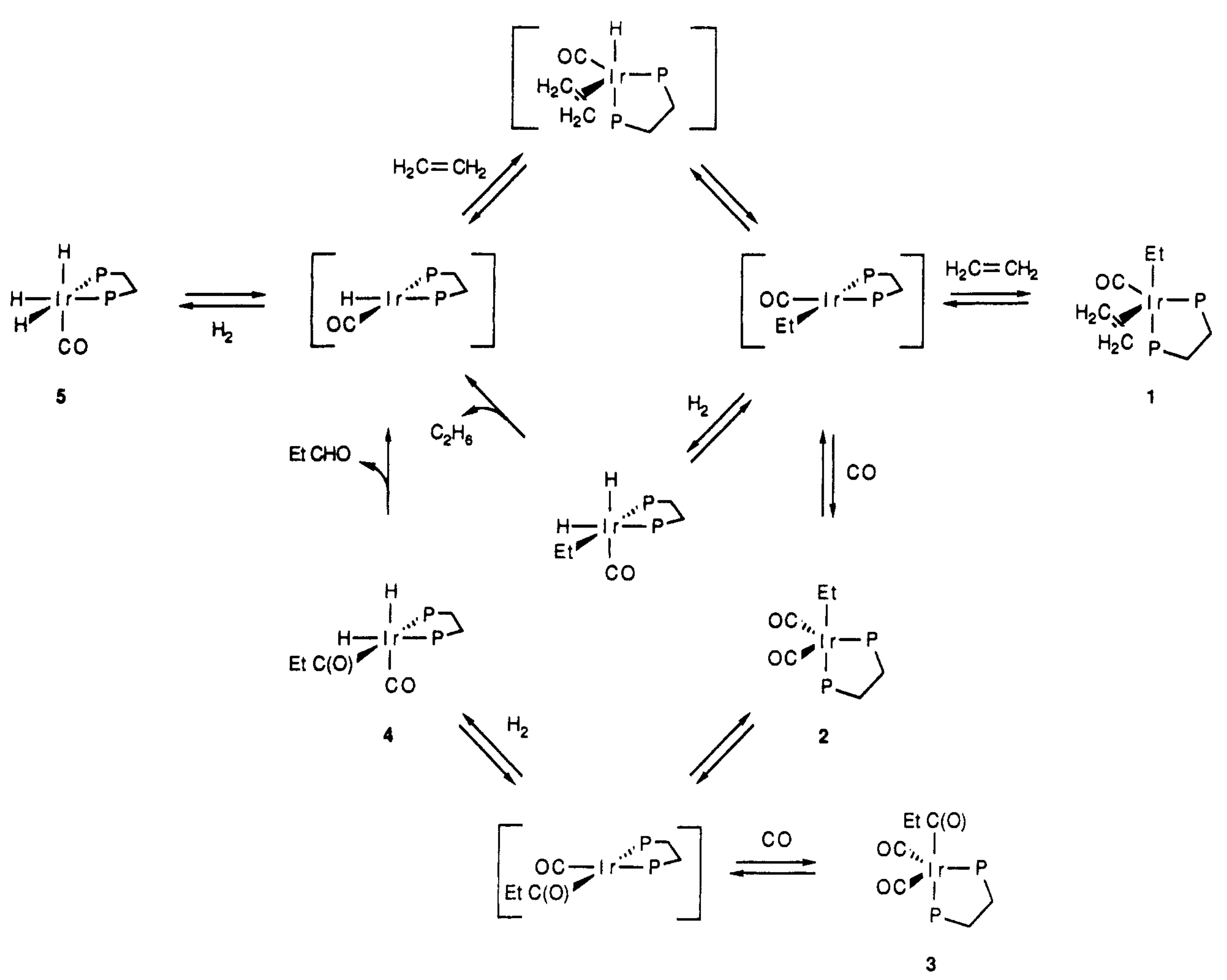

3.5 eu, respectively. Similar primary kinetic isotope effects were also observed with k_H/k_D (H-H/D-D) = 1.5 ± 0.1 for $IrH_2(C(O)Et)(CO)(dppe)$ and 1.6 ± 0.1 for $IrH_2(Et)(CO)(dppe)$. The small magnitude of the kinetic isotope effect for both H_2 elimination suggests net weakening of the M-H bonds in the transition states without H-H bond formation being fully compensating.

The reductive eliminations of EtCHO and H_2 from $IrH_2(C(O)Et)(CO)(dppe)$ as well as the reductive eliminations of EtH and H_2 from $IrH_2(Et)(CO)(dppe)$ all show significant negative values for $\Delta S^{\ddagger}$. While large negative values for $\Delta S^{\ddagger}$ usually imply associative reaction mechanisms,[27a] other experimental observations in the reductive elimination reactions of $IrH_2(C(O)Et)(CO)(dppe)$ and $IrH_2(Et)(CO)(dppe)$ argue against associative mechanisms. Specifically, (a) the reactions follow simple first-order kinetics, (b) their rates are independent of [Ir] and [H_2], and (c) values for k_{2f} are the same under both D_2 and CO. These observations indicate that both reductive eliminations occur by dissociative pathways. The negative $\Delta S^{\ddagger}$ values for the reductive eliminations indicate an ordered transition state for the reaction intermediates, but the basis of the ordering is unclear at this time.

There are far fewer acyl hydride transition metal complexes in the literature than there are alkyl hydride complexes. The result of this is that there are also far fewer kinetic studies of the reductive elimination of aldehydes from metal complexes despite the fact that this is a fundamental step in general catalytic hydroformylation and carbonylation mechanisms.

Milstein has reported on the synthesis and reactivity of *cis,mer*-$RhH(C(O)Me)(PMe_3)_3Cl$, formed by the oxidative addition of acetaldehyde to $Rh(PMe_3)_3Cl$. While the reductive elimination of acetaldehyde was intramolecular and followed first-order kinetics, phosphine dissociation to produce a 5-coordinate 16-electron rhodium(III) was the rate-determining initial step.[48a]

With the reductive elimination of EtCHO from 4 and the regeneration of $IrH_3(CO)(dppe)$, an iridium-catalyzed hydroformylation cycle has been completed. This cycle, shown in Scheme II, is very similar to those proposed for $RhH(CO)(PPh_3)_3$ and other monohydride complexes.[1-4,29a] Not all of the intermediates along the way have been observed, but precedent exists for those that are not observed in this particular case. The most important feature in this particular study, as far as the hydroformylation catalytic cycle is concerned, is the observation and characterization of the propionyl dihydride complex.

Concluding Remarks

Three complexes relevant to homogeneously catalyzed olefin hydroformylation have been prepared and characterized in this study: $Ir(Et)(CO)_2(dppe)$, $Ir(C(O)Et)(CO)_2(dppe)$, and $IrH_2(C(O)Et)(CO)(dppe)$. The last complex is the first well-documented example of an acyl dihydride species.

The facial arrangement of the propionyl and hydride ligands in $IrH_2(C(O)Et)(CO)(dppe)$ allows the competitive reductive eliminations of propionaldehyde and hydrogen to take place. The kinetics and mechanism of these internally competitive reductive eliminations were studied in detail. Both reactions occur through ordered transition states, with H–H elimination being more facile than EtC(O)–H elimination.

Experimental Section

All procedures were performed in a nitrogen-filled glovebox under nitrogen or other appropriate gas using a Schlenk-type vacuum line or on a high-vacuum line. Solutions for NMR samples were usually prepared in a glovebox and placed in resealable NMR tubes fitted with J. Young valves (Wilmad Glass Co.) or placed in NMR tubes attached to ground-glass joints and fitted with needle-valve adaptors for connection to a high-vacuum line. These NMR samples were connected to a high-vacuum line for freeze/pump/thaw cycles at −78 °C and/or exposure to gases, followed by sealing (or flame sealing). All solvents were reagent grade or better and were dried and degassed before use by accepted techniques.[49] Most gases were used as received, including hydrogen (Air Products, 99.9%), deuterium (Air Products, 99.99%), carbon monoxide (Air Products, CP 99.3%), and carbon-[^{13}C] monoxide (Monsanto Research Corp., 99%).

^{1}H and ^{31}P NMR spectra were recorded at 400.13 and 161.98 MHz, respectively, on a Bruker WH-400 spectrometer. A Bruker BVT-1000 temperature control unit was used in the regulation of temperature when needed and was calibrated against standard methanol (low temperature) or ethylene glycol (high temperature) samples. ^{13}C NMR spectra were recorded on a Nicolet QE-300 NMR at 75.48 MHz. ^{1}H chemical shifts are reported in ppm downfield from tetramethylsilane but were measured relative to residual ^{1}H resonances in the deuterated solvents C_6D_5H (δ 7.150) and $C_6D_5CD_2H$ (δ 2.100). ^{31}P chemical shifts are reported in ppm downfield from phosphoric acid and were referenced to external 85% H_3PO_4. ^{13}C chemical shifts are reported in ppm downfield from tetramethylsilane and were referenced to benzene-d_6 solvent (δ 127.6). Benzene-d_6 (MSD, 99.6% D) and toluene-d_8 (Aldrich, 99+% D) were vacuum distilled from sodium benzophenone ketyl solutions. Infrared spectra were recorded on a Mattson Sirius 100 FT-IR. Elemental analyses were performed by Galbraith Laboratories, Inc., Knoxville, TN.

The complexes $IrH_3(CO)(dppe)$,[40a] $Ir(Et)(\eta^2\text{-}C_2H_4)(CO)(dppe)$,[18] $IrH_3(^{13}CO)(dppe)$,[18] and $Ir(\eta^2\text{-}C_2H_4)(Et)(^{13}CO)(dppe)$[18] were prepared according to the literature procedures.

Reaction of $Ir(\eta^2\text{-}C_2H_4)(Et)(CO)(dppe)$ with CO. Formation of 2 and 3. In a typical reaction, 0.4 mL of a 10 mM benzene-d_6 solution of $Ir(Et)(\eta^2\text{-}C_2H_4)(CO)(dppe)$, **1**, was placed in a resealable NMR tube. After two freeze/pump/thaw cycles at −78 °C, the solution was frozen and pumped on at −78 °C, and the frozen solution placed under 400–700 Torr of CO. The reaction was then followed by NMR spectroscopy. The end product of this reaction, $Ir(C(O)Et)(CO)_2(dppe)$, can be prepared on a larger scale and isolated.

The reactions of ^{13}CO with $Ir(\eta^2\text{-}C_2H_4)(Et)(CO)(dppe)$ and $Ir(\eta^2\text{-}C_2H_4)(Et)(^{13}CO)(dppe)$ were performed by using a similar procedure.

Spectroscopic data for **2**: ^{1}H NMR (C_6D_6) δ 7.536 (dd, J = 10, 8 Hz, 8 H, dppe *o*-phenyl), 1.97 (br m, 4 H, dppe CH_2), 2.174 (br m, 3 H, CH_3CH_2–Ir), 2.09 (br m, 2 H, CH_3CH_2–Ir); $^{31}P\{^1H\}$ NMR (C_6D_6) δ 32.72 (br s), 30.428 (br s); IR ν_{CO} 1965, 1916 cm^{-1}. Spectroscopic data for ^{13}CO-labeled **2**: $^{13}C\{^1H\}$ NMR (C_6D_6) δ 187.84 (d, J = 28 Hz).

Spectroscopic data for **3**: ^{1}H NMR (C_6D_6) δ 7.740 (br s, 4 H, dppe *o*-phenyl), 7.434 (br s, 4 H; dppe *o*-phenyl), 1.94 (br m, 4 H, dppe CH_2), 2.830 (q, J = 7 Hz, 2 H, $CH_3CH_2C(O)$–Ir), 0.858 (t, J = 7 Hz, 3 H, $CH_3CH_2C(O)$–Ir); $^{31}P\{^1H\}$ NMR (C_6D_6) δ 25.85 (br s), 20.20 (br s); IR ν_{CO} = 1977, 1929, 1635 cm^{-1}. Spectroscopic data for ^{13}CO-labeled **3**: $^{13}C\{^1H\}$ NMR δ 186.81 (d, J_{C-P} = 23 Hz), 215.35 (d, J_{C-P} = 61 Hz); $^{31}P\{^1H\}$ NMR (C_6D_6) δ 25.85 (br s), 20.20 (d, $J_{C-P} \sim$ 70 Hz); IR ν_{CO} = 1925, 1878, 1588 cm^{-1}.

Preparation of $Ir(C(O)Et)(CO)_2(dppe)$, 3. $IrH_3(CO)(dppe)$ (105 mg, 0.169 mmol) dissolved in 2 mL of toluene was heated to 80 °C for 1 h under an atmosphere of ethylene, producing **1** in situ. After the solution cooled to room temperature, the ethylene atmosphere was replaced by carbon monoxide, and the solution was stirred for 12 h. Following the addition of 10 mL of absolute ethanol, the volume of the solution was reduced to 2 mL, resulting in the precipitation of a white powder, which was collected on a frit in air and washed with ethanol, yield 95 mg (80%). Anal. Calcd for $C_{31}H_{29}IrO_3P_2$: C, 52.91; H, 4.15. Found: C, 52.99; H, 4.11.

Reaction of $Ir(C(O)Et)(CO)_2(dppe)$ with H_2. Formation of 4. In a typical reaction, 0.4 mL of a 10 mM solution of $Ir(C(O)Et)(CO)_2(dppe)$ in benzene-d_6 was placed in a resealable NMR tube. After two freeze/pump/thaw cycles at −78 °C, the solution was frozen and pumped on at −78 °C, and the frozen solution placed under 400–700 Torr of H_2. The reaction was then followed by NMR spectroscopy. The end product of this reaction, $IrH_2(C(O)Et)(CO)(dppe)$, can also be prepared on a larger scale and isolated.

Spectroscopic data for **4**: ^{1}H NMR (C_6D_6) δ 8.051 (dd, J = 10, 9 Hz, 2 H, dppe *o*-phenyl), 7.909 (dd, J = 11, 8 Hz, 2 H, dppe *o*-phenyl), 7.603 (dd, J = 11, 8 Hz, 2 H, dppe *o*-phenyl), 7.332 (dd, J = 10, 7 Hz, 2 H, dppe *o*-phenyl), 2.20 (m, 1 H, dppe CH_2), 1.98 (m, 2 H, dppe CH_2), 1.84 (m, 1 H, dppe CH_2), 3.198 (dq, J = 16, 7 Hz, 1 H, one of two diastereotopic $CH_3CH_2C(O)$–Ir), 3.032 (dq, J = 16, 7 Hz, 1 H, one of two diastereotopic $CH_3CH_2C(O)$–Ir), 1.140 (t, J = 7 Hz, 3 H, $CH_3CH_2C(O)$–Ir), −8.473 (dd, J_{H-P} = 126, 14 Hz, 1 H, Ir–H), −8.795 (t, J_{H-P} = 20 Hz, 1 H, Ir–H); $^{31}P\{^1H\}$ (C_6D_6) δ 20.66 (d, J = 7 Hz), 19.74 (d, J = 7 Hz); IR (KBr) ν_{CO} = 1967, 1615 cm^{-1}, ν_{Ir-H} = 2066 cm^{-1}, other ν_{Ir-H} not located. **4**-d_2: IR ν_{CO} = 2013 cm^{-1}, ν_{IR-D} not located. Spectroscopic data for ^{13}CO-labeled **4**: $^{13}CO\{^1H\}$ NMR (C_6D_6) δ = 177.56 (br s) {in hydride-coupled spectrum: dd, J = 37, 4 Hz)}, 224.20 (d, J = 86 Hz) {in hydride-coupled spectrum: dd, J = 4, 4 Hz)}; ^{1}H NMR (C_6D_6) δ 3.198 (J_{H-C} = 4 Hz), 3.032 (J_{H-C} = 4 Hz), 1.140 (J_{H-C} = 5 Hz), −8.473 (J_{H-C} = 4, 4 Hz), −8.795 (J_{H-C} = 37, 3 Hz); $^{31}P\{^1H\}$ (C_6D_6) δ 19.74 (d, J_{P-C} = 86 Hz).

Preparation of $IrH_2(C(O)Et)(CO)(dppe)$, 4. A toluene solution (5 mL) of $Ir(C(O)Et)(CO)_2(dppe)$ (100 mg, 0.14 mmol) was stirred under an atmosphere of hydrogen at room temperature for 12 h. After the addition of 10 mL of absolute ethanol the solution was concentrated to 2 mL, giving a white solid, which was collected on a frit in air and washed with ethanol, yield 69 mg (72%). Anal. Calcd for $C_{30}H_{31}IrO_2P_2$: C, 53.16; H, 4.61. Found: C, 52.84; H, 4.66.

Kinetic Studies of the Reductive Eliminations from 4. In a nitrogen-filled glovebox, 0.40 mL of a freshly prepared ~5 mM stock solution of **4** in benzene-d_6 was added to each resealable NMR tube. The tubes were sealed, removed from the glovebox, and attached to a high-vacuum line. After undergoing a freeze/pump/thaw cycle at −196 °C to remove N_2, the tube was immersed in liquid nitrogen to just below the valve, and 700 Torr H_2 (or D_2, CO, or ^{13}CO) was added.[50]

The NMR tubes were thawed, vigorously shaken for 30 s, placed into the preheated NMR probe, and the reaction was monitored by ^{1}H NMR spectroscopy by following the decay of the hydride resonances of **4**. The decay of CH_2 resonances of the propionyl group of **4**, the growth of the hydride resonances attributed to $IrH_2(CO)(dppe)$, and the growth of the resonances attributed to free propionaldehyde were also monitored. For the reactions performed under H_2, the NMR tubes were periodically removed from the NMR probe and shaken vigorously to ensure mass transfer of H_2 between the gas and solution. For the reactions performed under D_2, the NMR tube was removed from the probe and shaken after each NMR accumulation (every 10 min) to ensure mass transfer of D_2 and H_2 between the gas and solution phases. The reactions were monitored for at least 2–4 half-lives. The reaction temperature ranged from 50.2 to 75.7 ± 0.3 °C.

X-ray Structure Determination of $Ir(C(O)Et)(CO)_2(dppe)$, 3. Colorless crystals of **3** were isolated from a saturated toluene solution at −30 °C. A parallelopiped crystal (0.1 × 0.2 × 0.3 mm) was attached to the end of a glass fiber with epoxy and mounted on a CAD4 kappa goniometer. The triclinic space group $P\bar{1}$ (no. 2) was determined by using the Enraf-Nonius CAD4-SDP peak search, centering, and indexing programs and was confirmed with the cell reduction program TRACER. Crystallographic data, experimental details of data collection, and structure refinement

---

(50) The total internal volume of the J. Young NMR tubes was ≃2.6 mL. With use of the ideal gas law with 2.2 mL of gas volume (0.4 mL solution), 700 mmHg, and −196 °C, there was ≃320 mmol of gas in the NMR tube or ≃150 equiv. The amount of gas in solution was however much smaller.

parameters for the crystal structure are presented in Table I and in Table S1 of the supplementary material (see the paragraph at the end of the paper). The intensity data for structure of 3 showed no evidence of decay upon X-ray irradiation. The structure was solved by standard heavy-atom methods with all remaining non-hydrogen atoms located through a succession of difference Fourier maps and least-squares refinements. In the final refinement model, all non-hydrogen atoms were refined anisotropically with hydrogen atoms placed at calculated positions. Table II contains the final refined positional and isotropic thermal parameters for the structure. The supplementary material contains the final anisotropic thermal parameters, the calculated hydrogen positional parameters, complete tabulations of bond distances and angles, and a listing of observed and calculated structure factor amplitudes for the structure.

Acknowledgment. We thank the National Science Foundation (CHE 86-03055 and 89-09060) for support of this work and the Johnson Matthey Co., Inc. for a generous loan of iridium trichloride. P.P.D. gratefully acknowledges Sherman Clarke and Elon Huntington Hooker Fellowships.

Supplementary Material Available: Tables of data collection and refinement parameters, final positional parameters, calculated hydrogen positional parameters, complete bond distances and angles, and anisotropic thermal parameters (11 pages); a listing of observed and calculated structure factors (22 pages). Ordering information is given on any current masthead page.

Catalytic Functionalization of C–H Bonds by Isonitrile Insertion. Preparation, Characterization, and Reactivity of $RhCl(PR_3)_2(CNR')$

William D. Jones*[,†] and Edward T. Hessell

Department of Chemistry, University of Rochester, Rochester, New York 14627

Received August 8, 1989

A series of complexes of the type *trans*-$RhCl(PR_3)_2(CNR')$, where R = Me, Et, *i*-Pr and R′ = neopentyl, 2,6-xylyl, or Me, have been prepared and examined for C–H bond activation. All of the neopentyl complexes produce 2,2-dimethyl-5-phenyl-4-aza-4-pentene (**5a**) upon irradiation in benzene solvent. In the presence of low concentrations of added isonitrile the production of **5a** is catalytic, with the R = isopropyl giving the highest yields. Two of the precursors were structurally characterized. The *trans*-$RhCl[P(i\text{-}Pr)_3]_2(CNCH_2CMe_3)$ (**2c**) crystallizes in the monoclinic space group $P2_1/c$ with $a = 13.894$ (5) Å, $b = 12.014$ (6) Å, $c = 18.896$ (9) Å, $\beta = 103.58$ (4)°, $V = 3066$ (5) Å^3, and $Z = 4$. The complex *trans*-$RhCl[P(i\text{-}Pr)_3]_2$(CN-2,6-xylyl) (**2e**) crystallizes in orthorhombic space group *Pnna* with $a = 14.620$ (2) Å, $b = 16.07$ (2) Å, $c = 15.358$ (4) Å, $V = 3608$ (5) Å^3, and $Z = 4$. At higher concentrations, a solution of **2c** and neopentyl isocyanide in benzene produces the complex $\{trans\text{-}Rh[P(i\text{-}Pr)_3]_2(CNCH_2CMe_3)_2\}^+Cl^-$ (**3a**), which precipitates from solution. Complex **3a** crystallizes in the monoclinic space group $P2_1/n$ with $a = 11.633$ (3) Å, $b = 13.945$ (3) Å, $c = 23.050$ (9) Å, $\beta = 92.69$ (2)°, $V = 3735$ (3) Å^3, and $Z = 4$. Complex **3a** is also found to serve as a catalyst for production of **5a**, but the PF_6^- salt **3b** is inactive.

Introduction

Saturated hydrocarbons are an abundant and inexpensive source of reduced carbon that would be suitable for use in the synthesis of organic compounds if it were not for their low reactivity. Methods presently used in industry for the functionalization of saturated hydrocarbons are typically inefficient, giving either a poor conversion of alkane or a lack of regioselectivity resulting in product mixtures.[1] The recent reports of the intermolecular activation of C–H bonds in alkanes by homogeneous transition-metal complexes, now becoming common in the chemical literature,[2] indicate that this reaction can be induced under mild thermal or photochemical homogeneous conditions with high regioselectivity.[3]

In spite of the recent increase in understanding the kinetics, thermodynamics, and mechanism(s) of this reaction,[4] the practical application of homogeneous C–H activation toward the development of a low-energy and selective alternative to the presently used industrial processes for the functionalization of saturated hydrocarbons remains a challenge for researchers. However, many significant advances have been recently achieved, most notably in the areas of alkane dehydrogenation[5,7] and carbonylation.[6,8] Both catalytic cycles suffer in that the overall reaction is thermodynamically unfavorable. In

---

[†] A. P. Sloan Fellow, 1984–86. Camille & Henry Dreyfus Teacher Scholar, 1985–89.

(1) Mortreux, A.; Petit, F. *Industrial Applications of Homogeneous Catalysis*; D. Reidel: Dordrecht, Holland, 1988.

(2) For recent reviews, see: Hill, C. L. *Activation and Functionalization of Alkanes*; Wiley: New York, 1989. Halpern, J. *Inorg. Chim. Acta* **1985**, *100*, 41–48. Crabtree, R. H. *Chem. Rev.* **1985**, *85*, 245–269. Shilov, A. E. *Activation of Saturated Hydrocarbons by Transition Metal Complexes*; D. Reidel: Boston, 1984.

(3) Bergman, R. G. *Science* **1984**, *223*, 902–223.

(4) Jones, W. D.; Feher, F. J. *Acc. Chem. Res.* **1989**, *22*, 91–100. Nolan, S. P.; Hoff, C. D.; Stoutland, P. O.; Newman, L. J.; Buchanan, J. M.; Bergman, R. G.; Yang, G. K.; Peters, K. S. *J. Am. Chem. Soc.* **1987**, *109*, 3143–3145. Jones, W. D.; Feher, F. J. *J. Am. Chem. Soc.* **1984**, *106*, 1650–1663. Jones, W. D.; Feher, F. J. *J. Am.* Chem. *Soc.* **1985**, *107*, 620–631. Wax, M. J.; Stryker, J. M.; Buchanan, J. M.; Kovac, C. A.; Bergman, R. G. *J. Am. Chem. Soc.* **1984**, *106*, 1121–1122. Buchanan, J. M.; Stryker, J. M.; Bergman, R. G. *J. Am. Chem. Soc.* **1985**, *107*, 1537–1550. Periana, R. A.; Bergman, R. G. *J. Am. Chem. Soc.* **1986**, *108*, 7332–7346.

(5) Baudry, D.; Ephritikhine, M.; Felkin, H.; Holmes-Smith, R. J. *J. Chem. Soc., Chem. Commun.* **1983**, 788–789. Burchard, T.; Felkin, H. *Nouv. J. Chim.* **1986**, *10*, 673–674. Burk, M. J.; Crabtree, R. H.; Parnell, C. P.; Uriate, R. J. *Organometallics* **1984**, *3*, 816–817. U.S. Patent No. US 4,670,621.

(6) (a) Sakakura, T.; Tanaka, M. *J. Chem. Soc., Chem. Commun.* **1987**, 758. (b) Sakakura, T.; Susaki, K.; Tokunaga, Y.; Wada, K.; Tanaka, M. *Chem. Lett.* **1988**, 155.

(7) Burk, M. J.; Crabtree, R. H. *J. Chem. Soc., Chem. Commun.* **1985**, 1829–1830. Sakakura, T.; Sodeyama, T.; Tokunaga, Y.; Tanaka, M. *Chem. Lett.* **1987**, 2211–2214. Sakakura, T.; Sodeyama, T.; Tokunaga, Y.; Tanaka, M. *Chem. Lett.* **1988**, 263–264.